JGR Biogeosciences

RESEARCH ARTICLE
10.1029/2022JG007159

Key Points:

- Fe(III) solubility was inferred from humic-like fluorescent dissolved organic matter
- Dissolved Fe concentration exceeded Fe(III) solubility in the intermediate water in the marginal seas
- Fe(III) solubility exceeded dissolved Fe concentration in the intermediate water away from the marginal seas

Correspondence to:

Y. Yamashita,
yamashiy@ees.hokudai.ac.jp

Citation:

Yamashita, Y., & Nishioka, J. (2023). Dissolved iron concentration and the solubility inferred by humic-like fluorescent dissolved organic matter in the intermediate water in the North Pacific including the marginal seas. *Journal of Geophysical Research: Biogeosciences*, *128*, e2022JG007159. https://doi.org/10.1029/2022JG007159

Received 29 AUG 2022
Accepted 13 FEB 2023

Author Contributions:

Conceptualization: Youhei Yamashita
Funding acquisition: Youhei Yamashita, Jun Nishioka
Investigation: Youhei Yamashita, Jun Nishioka
Visualization: Youhei Yamashita
Writing – original draft: Youhei Yamashita
Writing – review & editing: Youhei Yamashita, Jun Nishioka

Dissolved Iron Concentration and the Solubility Inferred by Humic-Like Fluorescent Dissolved Organic Matter in the Intermediate Water in the North Pacific Including the Marginal Seas

Youhei Yamashita[1] **and Jun Nishioka**[2]

[1]Faculty of Environmental and Earth Science, Hokkaido University, Sapporo, Japan, [2]Pan-Okhotsk Research Center, Institute of Low Temperature Science, Hokkaido University, Sapporo, Japan

Abstract The marginal seas have been found to be important external sources of dissolved iron (Fe) in the North Pacific through circulation of intermediate water. Here, we show comprehensive spatial distributions of dissolved Fe concentrations and Fe(III) solubilities inferred from humic-like fluorescent dissolved organic matter ($FDOM_H$) over the North Pacific, including the marginal seas, the Sea of Okhotsk, and the Bering Sea. $FDOM_H$ was used as a proxy of chemical speciation of dissolved Fe in the intermediate and deep waters where liner relationships were previously observed between $FDOM_H$ and Fe(III) solubility. When dissolved Fe concentration exceeds Fe(III) solubility, Fe(III) solubility is assumed to be equivalent to concentration of $FDOM_H$-Fe complexes, and excess dissolved Fe concentration above the Fe(III) solubility is assumed to be colloidal Fe which is not complexed with $FDOM_H$. In the intermediate water, the dissolved Fe concentration exceeded the Fe(III) solubility in the marginal seas, while excess Fe(III) solubility was evident downstream of the intermediate water circulation, suggesting that the major dissolved Fe chemical form derived from shelf and slope sediments in the marginal seas changed from colloidal Fe to $FDOM_H$-Fe complexes. With the previous findings, namely the dominance of labile particulate Fe in total Fe in the intermediate water of the Sea of Okhotsk and the Bering Sea, we hypothesized that the average size of sediment-derived Fe decreases during transportation by intermediate water, most likely due to reversible scavenging with the highest removal rate for labile particulate Fe and the lowest removal rate for $FDOM_H$-Fe complexes.

Plain Language Summary Iron (Fe) supply from the exterior of the ocean is important in sustaining global primary productivity. However, the distribution/strength of external sources and the mechanism for long-distance transport of dissolved Fe have not been well documented. We suggest that the major chemical form of marginal sea sediment-derived dissolved Fe changed from Fe colloids to soluble Fe during long-distance transport by the intermediate water of the North Pacific. The soluble Fe is likely dissolvable in seawater through forming complex with humic substances which are microbiologically and/or abiotically altered biogenic organic matter. This finding may help marine biogeochemical models better reproduce the Fe cycle.

1. Introduction

Iron (Fe) is a well-known micronutrient that controls the magnitude and dynamics of ocean primary productivity, particularly in high nutrient-low chlorophyll regions (Martin & Fitzwater, 1988). Since Fe is less soluble in oxic seawater (Kuma et al., 1996; Wu et al., 2001) and is scavenged from the water column, the flux and residence time of external Fe regulate ocean primary productivity (Boyd & Ellwood, 2010; Tagliabue et al., 2017). Although aeolian dust has been considered the major source of Fe in ocean primary productivity (Duce & Tindale, 1991; Johnson et al., 1997), hydrothermal vents and shelf sediments have also been thought important for global ocean primary productivity (Elrod et al., 2004; Johnson et al., 1999; Resing et al., 2015; Tagliabue et al., 2014). Since hydrothermal vents and shelf sediments are sporadically distributed in the global ocean, long-distance transport of Fe is vital for connecting external sources with primary productivity in remote ocean areas.

The chemical forms of measurable Fe in seawater are, in general, operationally defined as dissolved Fe (<0.2 μm) and labile particulate Fe (>0.2 μm) with filtration (e.g., Bruland & Rue, 2001). Furthermore, some studies separate dissolved Fe into soluble Fe and colloidal Fe by additional filtration with smaller pore sizes (i.e., 0.02,

0.03 μm, 200, and 1,000 kDa) (e.g., Nishioka et al., 2021b). Substantial fractions of dissolved Fe were found to be present in the colloid size fraction (Fitzsimmons & Boyle, 2014; Nishioka et al., 2003; Wu et al., 2001), and the contribution of colloidal Fe to the dissolved Fe content was thought to be highly variable across geographic locations and depths (von der Heyden & Roychoudhury, 2015). From the distributional pattern in a North Atlantic transect, Fitzsimmons et al. (2015) proposed a model for dissolved Fe size partitioning in which a "steady state" of dissolved Fe exchange reactions occurred during and following remineralization, including ligand exchange, sorption/desorption, and aggregation/disaggregation in the intermediate and deep waters, while soluble Fe and colloidal Fe appeared to cycle more independently in waters affected by external Fe sources. Additional knowledge regarding changes in the physicochemical speciation of dissolved Fe from external sources to remote oceans is needed to constrain the role of colloidal Fe in the ocean Fe cycle.

The major factor controlling dissolved Fe concentration above the thermodynamic solubility of Fe(III) in inorganic seawater is complexation with organic ligands (Kuma et al., 1996; Wu et al., 2001). The major organic ligands for Fe(III) have been considered to be siderophores which are products of a wide variety of bacteria, polysaccharides, and humic substances (Gledhill & Buck, 2012; Hassler et al., 2017). Humic substances have been defined as a general category of naturally occurring, biogenic, heterogeneous organic substances that can generally be characterized as being yellow to brown in color, of high molecular weight, and refractory (Aiken et al., 1985), even though recent studies pointed out that the high molecular weight is likely the result of supramolecular associations of relatively low molecular weight compounds (Romera-Castillo et al., 2014; Sutton & Sposito, 2005). Some chromophores which contribute to yellow to brown color are known to fluoresce, defined as humic-like or visible fluorescence (Coble, 1996, 2007; Stedmon & Nelson, 2015). On the other hand, in natural aquatic environments, the term of humic substances is often used for fractions, namely fulvic acids and humic acids, which is extracted from dissolved organic matter (DOM) with resins (e.g., XAD-8 resin) and separated with pH (Aiken, 1985). In marine environments, the term "humic ligands" is used to ligands determined by electroanalytical methods referred with humic fractions (e.g., Suwanee River Fulvic Acid and Suwanee River Humic Acid; Laglera et al., 2007; Laglera & van den Berg, 2009; Whitby & van den Berg, 2015), polydisperse ligands occurred throughout the water column (Boiteau et al., 2019), and humic-like fluorescent DOM ($FDOM_H$) which is linearly related to Fe(III) solubility in the dark ocean (Kitayama et al., 2009; Tani et al., 2003). The linkages among the three types of humic ligands have not been well documented. Although a strong correlation between humic ligands determined by an electroanalytical method and $FDOM_H$ was observed in the surface Arctic Ocean which is strongly influenced by riverine inputs (Laglera et al., 2019), no correlation between the two parameters was reported in the North Atlantic Ocean (Whitby et al., 2020b). It should be noted that both $FDOM_H$ and humic ligands determined by electroanalytical methods have been considered to be a mixture of allochthonous origin (e.g., riverine and sedimentary origins) and autochthonous origin which is produced with remineralization process (Whitby et al., 2020a, 2020b; Yamashita et al., 2020; Yamashita & Tanoue, 2008).

The western subarctic Pacific is connected with relatively large and deep marginal seas, namely, the Sea of Japan, the Sea of Okhotsk, and the Bering Sea. Recent studies showed that high levels of dissolved Fe and organic ligands, are transported from the Sea of Okhotsk and the Bering Sea to the western subarctic Pacific through circulation of intermediate water (Kondo et al., 2021; Nishioka et al., 2021a; Nishioka et al., 2013; Nishioka & Obata, 2017; Nishioka et al., 2020, 2007; Yamashita et al., 2020, 2021). The transportation of dissolved organic carbon and dissolved lignin, a biomarker of vascular plants, from the Sea of Okhotsk to the North Pacific by the intermediate water were observed (Hansell et al., 2002; Hernes & Benner, 2002). The long-distance transport was also suggested for dissolved trace elements, such as Zn, Mn, Hg, and Co (Hammerschmidt & Bowman, 2012; Kim et al., 2017; Laurier et al., 2004; Morton et al., 2019; Wong et al., 2022). Along 160°E line in the western North Pacific, Yamashita et al. (2020) directly compared the dissolved Fe concentration and Fe(III) solubility inferred from the abundance of $FDOM_H$ and suggested that dissolved Fe complexed with $FDOM_H$ is transported from the shelf sediments of the Sea of Okhotsk to the subtropical North Pacific, while colloidal Fe is probably scavenged during transportation. Although dissolved Fe was also reported to be transported from the Bering Sea to the western subarctic Pacific through circulation of the lower layer of intermediate water (Kondo et al., 2021; Nishioka & Obata, 2017), chemical speciation of dissolved Fe has not been clarified. Therefore, knowledge of the chemical forms of dissolved Fe throughout the North Pacific, including the subpolar marginal seas, is necessary to constrain the role of chemical forms in the long-distance transport of Fe in the North Pacific.

In this study, to understand the long-distance Fe transport mechanisms from the marginal seas to the whole North Pacific, we analyzed the dissolved Fe concentrations and $FDOM_H$ abundance that we have collected and

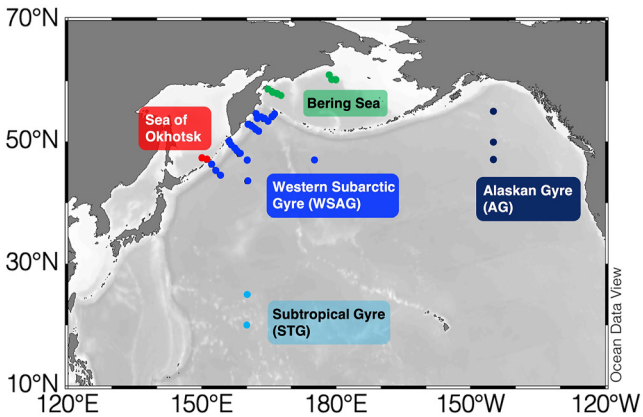

Figure 1. Map of the sampling sites in the basin regions.

reported so far (Nishioka et al., 2020; Yamashita et al., 2021). The Fe(III) solubility was estimated from $FDOM_H$ following the method proposed by Yamashita et al. (2020) and directly compared to the dissolved Fe concentration in the same sample. We expanded the survey region from a longitudinal transect reported by Yamashita et al. (2020) to a larger area over the North Pacific, including the marginal seas, that is, the Sea of Okhotsk and Bering Sea (Figure 1). We focused especially on changes in the chemical forms of dissolved Fe, namely, soluble Fe complexed with $FDOM_H$, colloidal Fe, labile particulate Fe (from the literature), and excess solubility by $FDOM_H$ from marginal seas to the remote North Pacific with circulation of intermediate water of the North Pacific.

2. Materials and Methods

The data and seawater samples used in this study were obtained during five field campaigns in July 2012 and June–August 2017 conducted by R/V *Hakuho Maru* (KH-12-3 and KH-17-3), in June–August 2014 and July–September 2017 conducted by R/V *Professor Multanovs*kiy (Mu14 and Mu18), and in August–September 2006 conducted by R/V *Professor Khromov* (Kh06; Figure 1). The basic oceanographic data, that is, temperature, salinity, density (σ_θ), dissolved oxygen concentration, and macronutrient concentrations, can be found elsewhere (Nishioka et al., 2020). N^*, a tracer of the influence of benthic denitrification, was calculated according to Yoshikawa et al. (2006);

$$N^* = \left([NO_3^-] + [NO_2^-] - 16 \times \left[PO_4^{3-}\right] + 2.9\right) \times 0.87 \quad (1)$$

The analytical procedure and data for dissolved Fe concentration are published and available in Nishioka et al. (2020). Briefly, the dissolved Fe concentration was analyzed for seawater filtered with an acid-cleaned 0.22 μm Millipak filter (Millipore) or 0.2 μm Acropak filter (Pall Company) using an FIA chemiluminescence detection system (Obata et al., 1993). All Fe data were obtained under GEOTRACES criteria.

The analytical procedure for $FDOM_H$ is described elsewhere (Yamashita et al., 2021). The samples collected during KH-12-3, Mu14, and Mu18 cruises were not filtered and measured onboard just after sampling. Other samples were filtered with acid-washed 0.22 (or 0.2) μm filters (Millipak or Acropak) and stored in freezer under dark condition until analysis in the laboratory on land. The fluorescence intensity for emission at 420 nm with 320 nm excitation was determined with a spectrofluorometer (RF-1500, Shimadzu or Fluoromax-4, Horiba) and calibrated to Raman units (RU_{320}, nm^{-1}) with the area under the water Raman peak of Milli-Q water (excitation = 320 nm). The filtration and freezing for preservation did not affect the fluorescence intensity of $FDOM_H$ (Yamashita et al., 2021). Some $FDOM_H$ data were reported in previous studies (Yamashita et al., 2020, 2021).

Fe(III) solubility was inferred from levels of $FDOM_H$ with the linear relationship between the two parameters in the deep waters (>1,000 m) of the Sea of Okhotsk and the western subarctic gyre (WSAG; Yamashita et al., 2020) as follows:

$$[\text{Fe(III) solubility}] = 96.2 \times [FDOM_H] \quad (2)$$

where the units of Fe(III) solubility and $FDOM_H$ are nM and RU_{320}, respectively. The error in the estimated Fe(III) solubility associated with conversion was approximately 10% (Yamashita et al., 2020). It was reported that relationships between Fe(III) solubility and $FDOM_H$ beneath the surface waters in the WSAG, the Sea of Japan, the Sea of Okhotsk, and the Bering Sea can be expressed by single linear regression (Takata et al., 2005), indicating that Fe(III) solubility in the intermediate and deep waters in the whole North Pacific including the marginal seas can be inferred from a linear regression between Fe(III) solubility and $FDOM_H$ (Equation 2).

In this study, the Fe(III) solubility inferred from $FDOM_H$ was used to define the abundance of organic-complexed Fe, which is in the soluble Fe concentration, and when the dissolved Fe concentration exceeds the solubility (excess Fe), the excess is defined as Fe in colloidal form (see Section 4, Discussion).

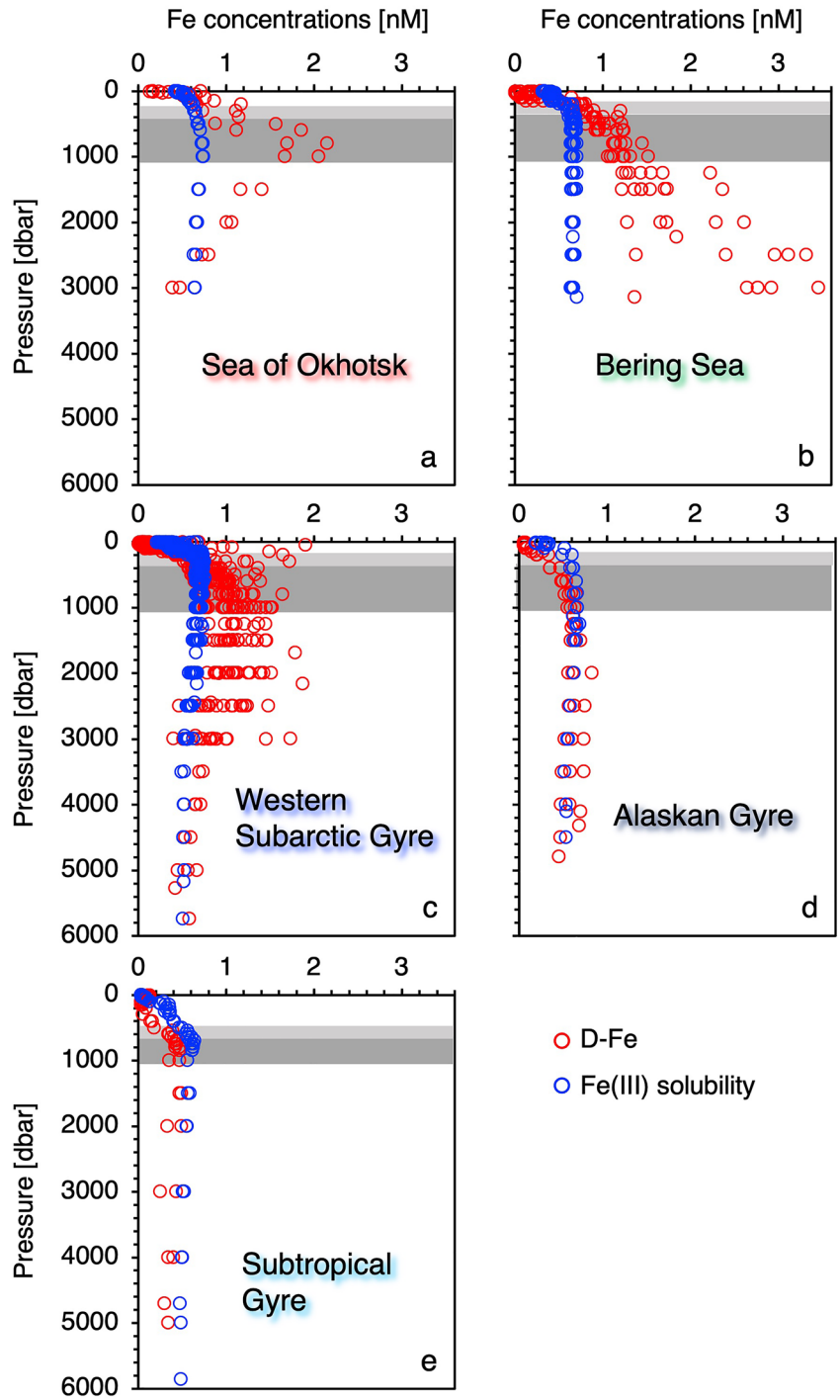

Figure 2. Vertical profiles for dissolved Fe concentration (red circles) and Fe(III) solubility (blue circles) in (a) the basin region of the Sea of Okhotsk, (b) the basin region of the Bering Sea, (c) the western subarctic gyre (WSAG), (d) the Alaskan gyre (AG), and (e) the subtropical gyre (STG). The light and dark gray areas correspond to the upper (26.6–27.0σ_θ) and lower intermediate waters (27.0–27.5σ_θ), respectively.

3. Results

3.1. Vertical Distributions of Dissolved Fe Concentration and Fe(III) Solubility

The dissolved Fe concentration was generally lowest in the surface water (Figure 2). However, the vertical patterns for dissolved Fe concentrations in the intermediate and deep waters largely differed among oceanic

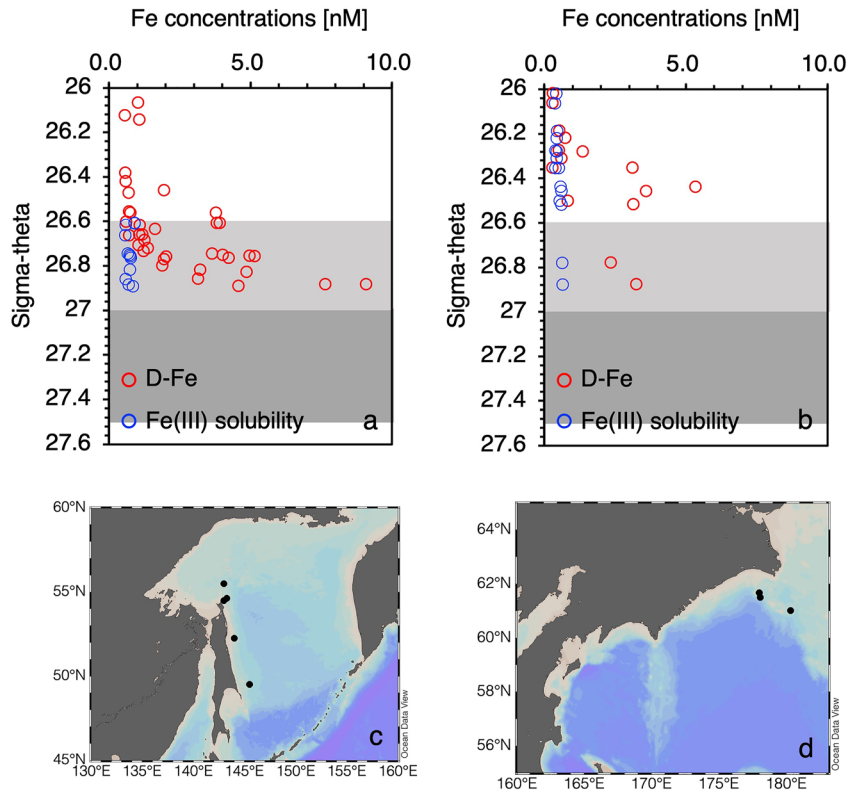

Figure 3. Relationships between sigma-theta and dissolved Fe concentration (red circles) as well as Fe(III) solubility (blue circles) at the shelf and slope regions in (a, c) the Sea of Okhotsk and (b, d) the Bering Sea. The water masses, whose densities were larger than 26.0σ_θ, are plotted in panels (a and b). The light and dark gray areas correspond to the upper (26.6–27.0σ_θ) and lower intermediate waters (27.0–27.5σ_θ), respectively.

regions (Figure 2). The levels of dissolved Fe in the upper and lower intermediate water (26.6–27.0σ_θ and 27.0–27.5σ_θ, respectively; Yasuda et al., 2001) in the basin region of the Sea of Okhotsk (Figure 2a), the basin region of the Bering Sea (Figure 2b), and the WSAG (Figure 2c) were higher than those in the Alaskan gyre (AG) (Figure 2d) and subtropical gyre (STG; Figure 2e). The levels of dissolved Fe in deep water (>27.5σ_θ) generally decreased with increasing water depth, except in the Bering Sea. In the Bering Sea, the levels of dissolved Fe in deep waters increased with increasing water depth.

The vertical patterns for Fe(III) solubility by $FDOM_H$ were similar among oceanic regions (Figure 2). The levels were lowest in the surface waters, increased with increasing water depths below the surface water, reached a maximum in the intermediate waters, and decreased slightly with increasing depths below the maximum. The dissolved Fe concentrations exceeded the Fe(III) solubility in numerous samples from the intermediate and deep waters in the Sea of Okhotsk, the Bering Sea, and the WSAG, while they were similar to or slightly lower than the Fe(III) solubility in samples from intermediate and deep waters in the AG and STG (Figure 2).

3.2. Dissolved Fe Concentration and Fe(III) Solubility in the Shelf and Slope Regions of Marginal Seas

Since dissolved Fe is laterally transported from the Sea of Okhotsk and the Bering Sea to the WSAG through intermediate water circulation (Kondo et al., 2021; Nishioka et al., 2021a; Nishioka et al., 2013, 2020; Yamashita et al., 2020), chemical speciation of the dissolved Fe in the shelf and slope of the marginal seas was determined for water masses >26.0σ_θ (Figure 3). The water mass corresponding to the lower intermediate water (27.0–27.5σ_θ) was not observed in the shelf and slope due to the relatively shallow bottom depth (~450 m).

The dissolved Fe concentration and Fe(III) solubility in the dense shelf water (DSW) and Okhotsk Sea Intermediate Water (OSIW; 26.6–27.0σ_θ) at the shelf and slope in the Sea of Okhotsk (~9 and 0.9 nM, respectively; Figure 3) were higher than those in the basin (Figure 2). The dissolved Fe concentration and Fe(III) solubility in

the upper intermediate water (26.6–27.0σ_θ) at the slope in the Bering Sea (~3 and 0.7 nM, respectively; Figure 3) were higher than and similar to those in the basin, respectively (Figure 2). The excess Fe concentrations compared with Fe(III) solubility in the upper intermediate water at the shelf and slope were higher than those at the basins in the Sea of Okhotsk and the Bering Sea.

4. Discussion

4.1. Possible Chemical Speciation of Dissolved Fe in the Intermediate and Deep Waters

It has been well documented that dissolved Fe concentration in marine environments exceeds thermodynamic solubility of Fe(III) in inorganic seawater due to existence of organic ligands (Kuma et al., 1996; Liu & Millero, 1999; Wu et al., 2001). Although the composition of organic ligands has not been well documented, siderophores (Boiteau et al., 2016, 2019), polysaccharides (Hassler et al., 2011), and humic substances (Boiteau et al., 2019; Laglera & van den Berg, 2009; Whitby et al., 2020b) are probable organic ligands in marine environments. The concentration of organic ligands determined by electroanalytical methods, for example, competitive ligand exchange-adsorptive cathodic stripping voltammetry (CLE-CSV), usually exceeds dissolved Fe concentration (Kondo et al., 2007). Recently, Whitby et al. (2020b) found that dissolved Fe concentrations did not significantly exceed the maximum potential Fe binding capacity of humic ligands determined by CSV from surface to deep waters, suggesting that upper limit of dissolved Fe concentration is controlled by complexation with humic ligands.

Kuma et al. (1996) determined Fe(III) solubility in seawater by adding radioactive ferric ^{59}Fe to the seawater, aging until saturated solution equilibrium, filtering with 0.025 μm filter, and measuring γ activity of ^{59}Fe in the filtrate. Strong linear relationships between Fe(III) solubility and $FDOM_H$ fluorescence intensity have been observed in wide areas of the North Pacific, including the marginal seas, except for surface waters (Kitayama et al., 2009; Takata et al., 2005; Tani et al., 2003; Yamashita et al., 2010). No correlation between Fe(III) solubility and $FDOM_H$ in surface waters is likely due to relatively large contribution of other organic ligands freshly produced by phytoplankton or bacteria, such as siderophores and polysaccharides (Heller et al., 2013; Takata et al., 2004). Since the siderophores and polysaccharides are generally microbiologically labile (Benner, 2011; Boiteau et al., 2016; Hassler et al., 2011, 2017), $FDOM_H$, which is photochemically labile but microbiologically recalcitrant (Yamashita & Tanoue, 2008), is likely the major factor controlling Fe(III) solubility in intermediate and deep waters. It should be noted that no correlation was observed between humic ligands concentration determined by CSV and $FDOM_H$ (Whitby et al., 2020b), suggesting that non-fluorescent humic ligands do not always correspond to the Fe(III) solubility but may complexed with Fe(III) in colloidal fraction as discussed below.

The probable molecular weight of $FDOM_H$ in the open ocean is less than 1.8 kDa (Omori et al., 2011), and size of $FDOM_H$ in 1 kDa–0.45 μm fraction at the Gulf of Mexico was estimated to be 0.5–4 nm (Stolpe et al., 2010). Fe(III) solubility corresponds to the upper limit of Fe concentration in the soluble fraction (<0.025 μm; Kuma et al., 1996). Such size characteristics of $FDOM_H$ and Fe(III) solubility suggests that the excess dissolved Fe concentration above the Fe(III) solubility in intermediate and deep waters likely occurs as colloidal Fe (0.025–0.2 μm) which is not complexed with $FDOM_H$ (Kitayama et al., 2009; Uchida et al., 2013; Yamashita et al., 2020). Our suggestion is probably reasonable, because the colloidal Fe has been observed ubiquitously from the surface to deep waters in the open ocean (Fitzsimmons et al., 2015; von der Heyden & Roychoudhury, 2015), including the WSAG and AG (Kondo et al., 2021; Nishioka et al., 2003).

Hereafter, we used $FDOM_H$ as a proxy of chemical speciation of dissolved Fe. $FDOM_H$-Fe complex concentration is equivalent with Fe(III) solubility assuming that all $FDOM_H$ complexes with Fe(III) when the dissolved Fe concentration exceeds the Fe(III) solubility. When the dissolved Fe concentration exceeds the Fe(III) solubility, the concentration of colloidal Fe, which is not complexed with $FDOM_H$, was estimated as the difference between the dissolved Fe concentration and Fe(III) solubility (Yamashita et al., 2020). On the other hand, when the Fe(III) solubility exceeds the dissolved Fe concentration, excess solubility inferred by $FDOM_H$ was calculated as the difference between Fe(III) solubility and the dissolved Fe concentration. The limitation of the proxy is that non-fluorescent DOM that exhibits the same behavior as $FDOM_H$ in the <0.025 μm fraction is counted as $FDOM_H$-Fe complex. The production of strong as well as weak Fe-binding ligands, including humic ligands determined by CSV and siderophores, were observed during remineralization experiments of particulate organic matter (Boyd et al., 2010; Bundy et al., 2016; Velasquez et al., 2016; Whitby et al., 2020a). Since $FDOM_H$ is also

produced during remineralization of particles (Yamashita & Tanoue, 2004, 2008), these Fe-binding ligands can contribute Fe(III) solubility if these ligands are microbiologically recalcitrant, thus, $FDOM_H$ proxy as a Fe(III) solubility may account for mixture of Fe-binding ligands produced during remineralization of particles. Alternatively, remineralization derived Fe-binding ligands excepting the $FDOM_H$ may be complexed with colloidal Fe. The latter mechanism is feasible, because organic ligands were observed not only soluble fraction but also colloidal fraction in the intermediate waters in the WSAG and AG (Kondo et al., 2021).

4.2. Changes in Possible Chemical Forms of Dissolved Fe During the Transportation Through Intermediate Water Circulation

The levels of $FDOM_H$-Fe complexes were generally lowest in the surface water, increased with depth beneath the surface water, showed maximum in the intermediate water, and does not change largely or slightly decrease with deep in the deep waters, irrespective of differences in oceanic regions (Figure 4). Similar vertical and spatial patterns with $FDOM_H$-Fe complexes (namely, Fe(III) solubility) were observed for Fe(III) solubility in the North Pacific (Kitayama et al., 2009). On the one hand, the level of $FDOM_H$ is mainly controlled by photobleaching by sunlight (Helms et al., 2013; Mopper et al., 1991; Omori et al., 2011; Timko et al., 2015). On the other hand, $FDOM_H$ is usually linearly related to apparent oxygen utilization (AOU) in intermediate and deep waters, indicating that biologically recalcitrant $FDOM_H$ is produced in situ as organic matter is biologically oxidized (Catalá et al., 2015; Jørgensen et al., 2011; Yamashita & Tanoue, 2008). Thus, in general, the level of $FDOM_H$-Fe complexes in the intermediate water and deep waters is likely controlled by microbial production of $FDOM_H$ during the remineralization. The microbial production of Fe-binding (humic) ligands in the dark ocean has also been pointed out by the electroanalytical methods and liquid chromatography-inductively coupled mass spectrometry (Boiteau et al., 2019; Boyd & Ellwood, 2010; Boyd et al., 2010; Whitby et al., 2020b).

The deviations from the linear relationship between $FDOM_H$ and AOU were observed in the North Pacific Intermediate Water (NPIW; Yamashita et al., 2020; Yamashita & Tanoue, 2008) and the North Atlantic Deep Water (Catalá et al., 2015; Jørgensen et al., 2011). In the case of the North Pacific, the deviations were attributed to allochthonous $FDOM_H$ derived from shelf sediments of the Sea of Okhotsk (Yamashita et al., 2020), and the allochthonous $FDOM_H$ was found to be transported conservatively over the North Pacific through the circulation of intermediate water (Yamashita et al., 2021). Thus, $FDOM_H$-Fe(III) complexes can be separated into autochthonous complexes and allochthonous complexes (Yamashita et al., 2020).

The allochthonous $FDOM_H$ supplied by formation of the DSW (Yamashita et al., 2020) likely contributes slightly higher levels of Fe(III) solubility in the upper intermediate water on the shelf and slope compared with the basin of the Sea of Okhotsk (Figures 2 and 3). However, colloids are the major chemical form of dissolved Fe in the water mass (0.2–8.4 nM; Figure 3). The dominance of colloidal Fe in dissolved Fe has also been observed in water masses affected by sedimentary resuspension along the western Atlantic margin (Fitzsimmons et al., 2015). High levels of colloidal Fe and labile particulate Fe are distributed in the DSW, OSIW, and upper intermediate water in the WSAG (Lam & Bishop et al., 2008; Nishioka et al., 2014, 2007). The labile particulate Fe was suggested to be sourced from redox-driven remobilization and subsequent formation of micron-sized Fe (oxyhydr)oxides and Fe bearing volcanic minerals such as olivines and pyroxenes at shelf and upper slope sediments (Lam & Bishop et al., 2008). On the other hand, the dissolved Fe flux from sediments to the water column was found to be correlated with oxidation of organic matter, and thus, high fluxes were observed for the high-productivity continental shelf (Elrod et al., 2004). When oxygen is consumed during the oxidation of organic matter within surface sediments, microbial Fe reduction becomes a favorable metabolic pathway. The Fe(II) formed under anoxic conditions diffuses into oxic areas, is oxidized to Fe(III), and reprecipitates (Lohan & Bruland, 2008). Conversely, Fe(III), which complexes with organic ligands, can be dissolved and transported to the water column (Lohan & Bruland, 2008). N^* for the DSW and OSIW observed in this study ranged from −6 to −14, which indicated the influence of denitrification in anoxic shelf sediments (Nishioka et al., 2007; Yoshikawa et al., 2006), suggesting that the allochthonous $FDOM_H$-Fe complexes likely formed through oxidation of anoxic sediments during a resuspension event accompanying the formation of the DSW (Nakatsuka et al., 2002, 2004). Thus, colloidal Fe complexed with and/or incorporated into organic (macro)molecules excepting $FDOM_H$ may also be formed during the oxidation process and transported to the water column.

The major fraction of $FDOM_H$ in the intermediate water of the Bering Sea was found to be autochthonous $FDOM_H$ (Yamashita et al., 2021). The higher levels of dissolved Fe in the upper intermediate water in the slope

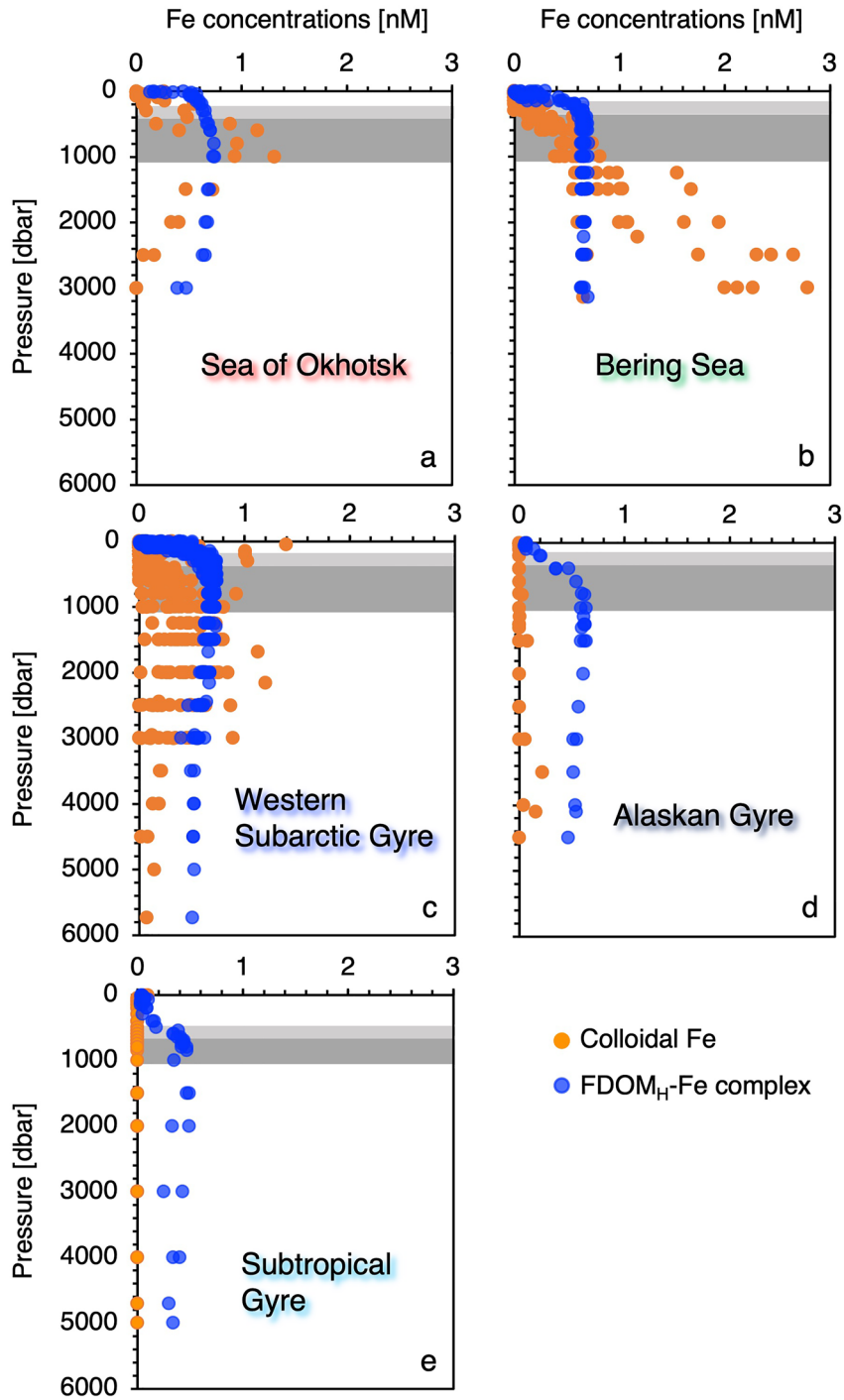

Figure 4. Vertical profiles for colloidal Fe concentration (orange circles) and $FDOM_H$-Fe complexes (blue circles) in (a) the basin region of the Sea of Okhotsk, (b) the basin region of the Bering Sea, (c) the western subarctic gyre (WSAG), (d) the Alaskan gyre (AG), and (e) the subtropical gyre (STG). The light and dark gray areas correspond to the upper (26.6–27.0σ_θ) and lower intermediate waters (27.0–27.5σ_θ), respectively.

compared with the basin of the Bering Sea (Figures 2 and 3) indicate that dissolved Fe dominated by colloidal Fe is supplied from slope sediments. The N^* values of the water masses were −2 and were similar to that of the upper intermediate water in the basin of the Bering Sea (Nishioka et al., 2021a), implying that the dissolved Fe in the upper intermediate water was possibly derived from oxic environments in the slope sediments in the Bering Sea. Since autochthonous $FDOM_H$ is most likely produced during oxidation of sedimentary organic matter in

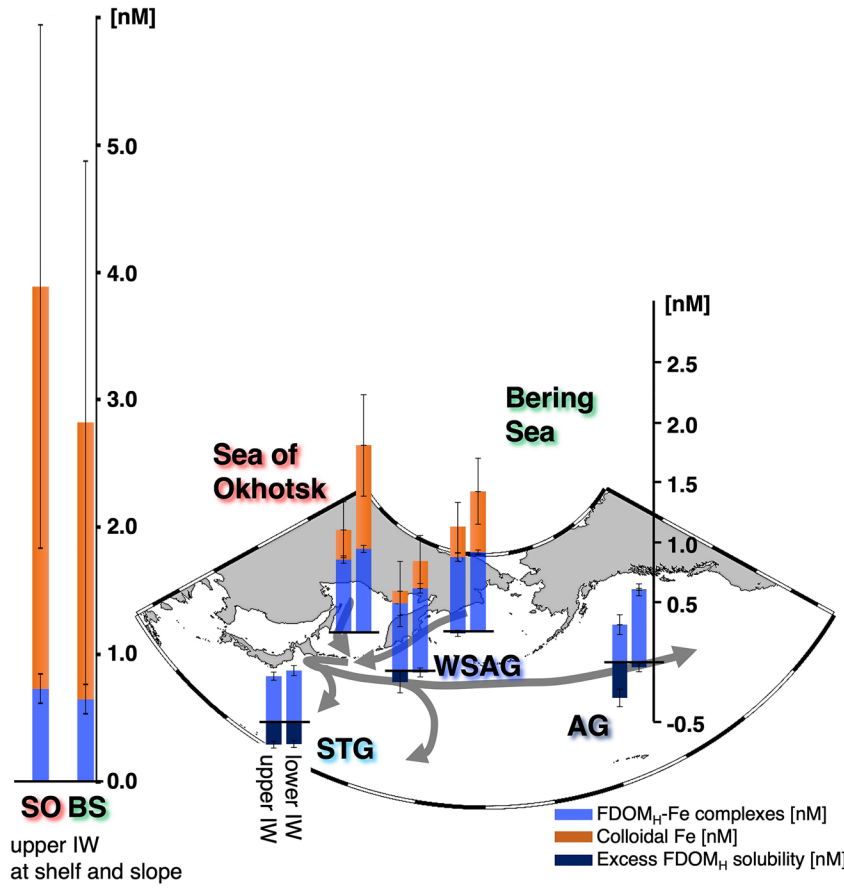

Figure 5. Spatial distributions of the $FDOM_H$-Fe complex (blue), colloidal Fe (orange), and excess $FDOM_H$ solubility (dark blue) in the upper intermediate waters (upper IW, left) and lower intermediate waters (lower IW, right) in basin regions in the North Pacific (western subarctic gyre, WSAG; Alaskan Gyre, AG; subtropical gyre, STG) and marginal seas and in the shelf and slope regions in the Sea of Okhotsk (SO) and the Bering Sea (BS). The color and error bars represent the average and standard deviation. The gray arrows show a schematic pathway for intermediate water circulation.

oxic sediments, oxic environments in slope sediments possibly supply autochthonous $FDOM_H$-Fe complexes as well as colloidal Fe.

The upper and lower NPIW was determined to be mainly derived from the Sea of Okhotsk and the Bering Sea, respectively (Yasuda et al., 2001). The high levels of dissolved Fe in the intermediate water of the WSAG were pointed out to be the result of lateral inputs from the Sea of Okhotsk and the Bering Sea (Kondo et al., 2021; Nishioka et al., 2021a; Nishioka et al., 2013; Nishioka & Obata, 2017; Nishioka et al., 2020; Yamashita et al., 2020). To better illustrate the changes in the major chemical form of dissolved Fe from marginal seas to the North Pacific along with the circulation of intermediate water, the $FDOM_H$-Fe complex concentration, colloidal Fe concentration, and excess $FDOM_H$ solubility were averaged in the upper and lower intermediate waters for each oceanic region (Figure 5). Furthermore, the relative abundances (%) of colloidal Fe and $FDOM_H$-Fe complexes in total dissolved Fe (namely colloidal Fe + $FDOM_H$-Fe complexes) were calculated for each sample, and then, were averaged for each water mass in each oceanic region. Colloidal Fe contributed 74% ± 20% (n = 12) and 73%–80% (n = 2) of the dissolved Fe in the upper intermediate water at the shelf and slope in the Sea of Okhotsk and the Bering Sea, respectively (Figure 5). The major form of dissolved Fe in the upper intermediate water at the basin regions is, however, $FDOM_H$-Fe complexes. The $FDOM_H$-Fe complexes contributed 76% ± 18% (n = 5) and 74% ± 16% (n = 14) of the dissolved Fe in the upper intermediate water in the basin region in the Sea of Okhotsk and the Bering Sea respectively, while it contributed 92% ± 17% (n = 47) in the WSAG and 100% ± 0% (n = 3) and 100% ± 0% (n = 3) in the AG and STG respectively. The excess $FDOM_H$ solubility is evident in the intermediate water in the STG and AG, far from the marginal seas.

Yamashita et al. (2020) pointed out that the major chemical form of dissolved Fe in the upper intermediate water changed from colloidal Fe to allochthonous $FDOM_H$-Fe complexes during long-distance transport of sediment-derived dissolved Fe from the Sea of Okhotsk to the STG. The present study showed that the dissolved Fe in the upper intermediate water in the AG is $FDOM_H$-Fe complexes but not the colloidal Fe (Figures 4 and 5). The allochthonous $FDOM_H$ was also observed in the upper intermediate water in the AG (Yamashita et al., 2021). These results suggest that change in the major chemical form of shelf sediment-derived dissolved Fe from colloidal Fe to $FDOM_H$-Fe complex probably occurred along the pathway of intermediate water circulation, not only to the south, the STG, but also to the east, the AG. However, it should be noted that colloidal Fe and ligands were observed after sequential filtration in the intermediate water not only in the WSAG but also in the AG (Kondo et al., 2021), implying that non-fluorescent colloidal ligands may also be a factor influencing chemical speciation of dissolved Fe.

The concentrations of colloidal Fe and $FDOM_H$-Fe complexes in the upper and lower intermediate waters in the Bering Sea were higher than and similar to those in the WSAG, respectively (Figures 4 and 5). The major origins of upper intermediate water (i.e., the Sea of Okhotsk) and lower intermediate water (i.e., the Bering Sea; Yasuda et al., 2001) suggest that both forms of dissolved Fe from the Bering Sea may not be contributed to those in the upper intermediate water but may be contributed to those in the lower intermediate water in the WSAG. A vertical descent of the dissolved Fe concentration peak in the hydrothermal plume during long-distance transport from the hydrothermal vent was interpreted as reversible exchange with a gravitationally sinking particulate phase through rapid adsorption/desorption, aggregation/disaggregation, and ligand exchange (Fitzsimmons et al., 2017). Thus, colloidal Fe in the lower intermediate water in the WSAG may also be the result of the vertical Fe descent with reversible scavenging of sediment-derived Fe.

The levels of labile particulate Fe were two orders of magnitude higher than those of dissolved Fe in the DSW in the Sea of Okhotsk (Nishioka et al., 2014). The levels of labile particulate Fe were also several times higher than those of dissolved Fe in the upper intermediate water in the Bering Sea (Nishioka et al., 2021a). Such high levels of labile particulate Fe in the upper intermediate water in the marginal seas were probably derived from shelf/slope sediments, as discussed above. The ratio of labile particulate Fe to dissolved Fe in the intermediate water in the subarctic Pacific was smaller than that in the Bering Sea (Uchida et al., 2013). In addition, the ratio in the upper intermediate water decreased from west to the east in the North Pacific (Kitayama et al., 2009; Uchida et al., 2013). In summary, the ratio of labile particulate Fe to dissolved Fe in the intermediate water decreases in the order marginal seas (the Sea of Okhotsk and the Bering Sea) > WSAG > AG and STG, that is, decreases with the pathway of intermediate water circulation. Similarly, the colloidal Fe concentration in the upper intermediate water was highest in the marginal seas and lowest in the AG and STG, while the $FDOM_H$-Fe complexes in the upper intermediate water were relatively uniformly distributed (Figures 4 and 5). Based on the distributional patterns of labile particulate Fe (summarized above), colloidal Fe and $FDOM_H$-Fe complexes (Figures 4 and 5), we can hypothesize that the average size of sediment-derived Fe decreases during transportation by intermediate water, most likely due to scavenging with the highest removal rate for labile particulate Fe and the lowest removal rate for $FDOM_H$-Fe complexes.

5. Concluding Remarks

The chemical speciation of dissolved Fe, namely colloidal Fe versus $FDOM_H$-Fe complexes, in the intermediate water in the North Pacific and the marginal seas is discussed with dissolved Fe concentration and Fe(III) solubility inferred from $FDOM_H$. With the previously reported distributional patterns of labile particulate Fe, the changes in the major chemical form of shelf sediment-derived Fe during intermediate water circulation was hypothesized to be changed from predominance of labile particulate Fe to $FDOM_H$-Fe complexes via colloidal Fe. To confirm the hypothesis, the simultaneous observation of size fractionated Fe and $FDOM_H$ (particulate, colloidal, and soluble fractions) from the marginal seas to the North Pacific is necessary. Addition of size fractionated humic ligands determined by an electroanalytical method to the simultaneous observation is effective to constrain the linkage between the humic ligands and $FDOM_H$.

Misumi et al. (2021) successfully reproduced the distributions of dissolved Fe in the North Pacific with a marine biogeochemical model implemented with dissolved Fe inputs from shelf sediments of the Sea of Okhotsk and the Bering Sea and reversible exchange of Fe between dissolved and slowly sinking particulate phases with constant concentrations of organic ligands. Recent studies (e.g., Fitzsimmons et al., 2015; Tagliabue et al., 2019),

including this study (Figure 5), suggest that Fe-binding ligands such as $FDOM_H$ are an important factor shaping the distribution of dissolved Fe but that other factors involved in the production of particulate and colloidal forms with reversible scavenging are also coregulated. This study suggests that the addition of reversible exchange among labile particulate Fe, colloidal Fe possibly complexed with organic ligands, and soluble Fe complexed with $FDOM_H$ to a marine biogeochemical model may lead to better reproduction of dissolved Fe concentrations in the ocean.

Data Availability Statement

The data used for this study, except those for $FDOM_H$, are available at Hokkaido University Collection of Scholarly and Academic Papers (HUSCAP) via http://hdl.handle.net/2115/77482. All data used in this study are available at HUSCAP via http://hdl.handle.net/2115/85729.

Acknowledgments
The authors would like to thank the captain, crew, and scientists onboard the R/V *Hakuho Maru*, R/V *Professor Multanovs*kiy, and R/V *Professor Khromov* for their help with observations. The authors are grateful to Dr. Y. Volkov, director of the Far Eastern Hydrometeorological Research Institute, for conducting the Japanese-Russian joint research program. This work was supported by the Japan Society for the Promotion of Science Grants KAKENHI (JP18H04910 and JP19H04250 to Youhei Yamashita, JP20K21838, JP21H05056, and JP22H05205 to Jun Nishioka). This study was supported in part by a Grant for Joint Research Program of the Institute of Low Temperature Science, Hokkaido University.

References

Aiken, G. R. (1985). Isolation and concentration techniques for aquatic humic substances. In D. M. McKnight, R. L. Wershaw, & P. MacCarthy (Eds.), *Humic substances in soil, sediment, and water: Geochemistry, isolation, and characterization* (pp. 363–385). John Wiley & Sons.

Aiken, G. R., McKnight, D. M., Wershaw, R. L., & MacCarthy, P. (1985). An introduction to humic substances in soil, sediment, and water. In D. M. McKnight, R. L. Wershaw, & P. MacCarthy (Eds.), *Humic substances in soil, sediment, and water: Geochemistry, isolation, and characterization* (pp. 1–9). John Wiley & Sons.

Benner, R. (2011). Loose ligands and available iron in the ocean. *Proceedings of the National Academy of Sciences of the United States of America*, *108*(3), 893–894. https://doi.org/10.1073/pnas.1018163108

Boiteau, R. M., Mende, D. R., Hawco, N. J., McIlvin, M. R., Fitzsimmons, J. N., Saito, M. A., et al. (2016). Siderophore-based microbial adaptations to iron scarcity across the eastern Pacific Ocean. *Proceedings of the National Academy of Sciences of the United States of America*, *113*(50), 14237–14242. https://doi.org/10.1073/pnas.1608594113

Boiteau, R. M., Till, C. P., Coale, T. H., Fitzsimmons, J. N., Bruland, K. W., & Repeta, D. L. (2019). Patterns of iron and siderophore distributions across the California Current System. *Limnology & Oceanography*, *64*(1), 376–389. https://doi.org/10.1002/lno.11046

Boyd, P. W., & Ellwood, M. J. (2010). The biogeochemical cycle of iron in the ocean. *Nature Geoscienc*e, 3(10), 675–682. https://doi.org/10.1038/ngeo964

Boyd, P. W., Ibisanmi, E., Sander, S. G., Hunter, K. A., & Jackson, G. A. (2010). Remineralization of upper ocean particles: Implications for iron biogeochemistry. *Limnology & Oceanography*, *55*(3), 1271–1288. https://doi.org/10.4319/lo.2010.55.3.1271

Bruland, K. W., & Rue, E. L. (2001). Analytical methods for the determination of concentrations and speciation of iron. In D. R. Turner, & K. A. Hunter (Eds.), *Biogeochemistry of Fe in seawater, SCOR-IUPAC series* (pp. 255–289). John Wiley.

Bundy, R. M., Jiang, M., Carter, M., & Barbeau, K. A. (2016). Iron-binding ligands in the southern California Current System: Mechanistic studies. *Frontiers in Marine Science*, *3*, 27. https://doi.org/10.3389/fmars.2016.00027

Catalá, T. S., Reche, I., Fuentes-Lema, A., Romera-Castillo, C., Nieto-Cid, M., Ortega-Retuerta, E., et al. (2015). Turnover time of fluorescent dissolved organic matter in the dark global ocean. *Nature Communications*, *6*(1), 5986. https://doi.org/10.1038/ncomms6986

Coble, P. G. (1996). Characterization of marine and terrestrial DOM in seawater using excitation-emission matrix spectroscopy. *Marine Chemistry*, *51*(4), 325–346. https://doi.org/10.1016/0304-4203(95)00062-3

Coble, P. G. (2007). Marine optical biogeochemistry: The chemistry of ocean color. *Chemical Reviews*, *107*(2), 402–418. https://doi.org/10.1021/cr050350+

Duce, R. A., & Tindale, N. W. (1991). Atmospheric transport of iron and its deposition in the ocean. *Limnology & Oceanography*, *36*(8), 1715–1726. https://doi.org/10.4319/lo.1991.36.8.1715

Elrod, V. A., Berelson, W. M., Coale, K., & Johnson, K. S. (2004). The flux of iron from continental shelf sediment: A missing source for global budget. *Geophysical Research Letters*, *31*, L12307. https://doi.org/10.1029/2004GL020216

Fitzsimmons, J. N., & Boyle, E. A. (2014). Both soluble and colloidal iron phases control dissolved iron variability in the tropical North Atlantic Ocean. *Geochimica et Cosmochimica Acta*, *125*, 539–550. https://doi.org/10.1016/j.gca.2013.10.032

Fitzsimmons, J. N., Carrasco, G. G., Wu, J., Roshan, S., Hatta, M., Measures, C. I., et al. (2015). Partitioning of dissolved iron and iron isotopes into soluble and colloidal phases along the GA03 GEOTRACES North Atlantic Transect. *Deep-Sea Research II*, *116*, 130–151. https://doi.org/10.1016/j.dsr2.2014.11.014

Fitzsimmons, J. N., John, S. G., Marsay, C. M., Hoffman, C. L., Nicholas, S. L., Toner, B. M., et al. (2017). Iron persistence in a distal hydrothermal plume supported by dissolved-particulate exchange. *Nature Geoscience*, *10*(3), 195–201. https://doi.org/10.1038/ngeo2900

Gledhill, M., & Buck, K. M. (2012). The organic complexation of iron in the marine environment: A review. *Frontiers in Microbiology*, *3*, 69. https://doi.org/10.3389/fmicb.2012.00069

Hammerschmidt, C. R., & Bowman, K. L. (2012). Vertical methylmercury distribution in the subtropical North Pacific Ocean. *Marine Chemistry*, *132–133*, 77–82. https://doi.org/10.1016/j.marchem.2012.02.005

Hansell, D. A., Carlson, C. A., & Suzuki, Y. (2002). Dissolved organic carbon export with North Pacific Intermediate Water formation. *Global Biogeochemical Cycles*, *16*(1), 7-1–7-8. https://doi.org/10.1029/2000gb001361

Hassler, C. S., Schoemann, V., Nichols, C. M., Butler, E. C. V., & Boyd, P. W. (2011). Saccharides enhance iron bioavailability to Southern Ocean phytoplankton. *Proceedings of the National Academy of Sciences of the United States of America*, *108*(3), 1076–1081. https://doi.org/10.1073/pnas.1010963108

Hassler, C. S., van den Berg, C. M. G., & Boyd, P. W. (2017). Toward a regional classification to provide a more inclusive examination of the ocean biogeochemistry of iron-binding ligands. *Frontiers in Marine Science*, *4*, 19. https://doi.org/10.3389/fmars.2017.00019

Heller, M. I., Gaiero, D. M., & Croot, P. L. (2013). Basin scale survey of marine humic fluorescence in the Atlantic: Relationship to iron solubility and H_2O_2. *Global Biogeochemical Cycles*, *27*(1), 88–100. https://doi.org/10.1029/2012gb004427

Helms, J. R., Stubbins, A., Perdue, E. M., Green, N. W., Chen, H., & Mopper, K. (2013). Photochemical bleaching of oceanic dissolved organic matter and its effect on absorption spectral slope and fluorescence. *Marine Chemistry*, *155*, 81–91. https://doi.org/10.1016/j.marchem.2013.05.015

Hernes, P. J., & Benner, R. (2002). Transport and diagenesis of dissolved and particulate terrigenous organic matter in the North Pacific Ocean. *Deep-Sea Research Part I*, *49*(12), 2119–2132. https://doi.org/10.1016/s0967-0637(02)00128-0

Johnson, K. S., Chavez, F. P., & Friederich, G. E. (1999). Continental-shelf sediment as a primary source of iron for coastal phytoplankton. *Nature*, *398*(6729), 697–700. https://doi.org/10.1038/19511

Johnson, K. S., Gordon, R. M., & Coale, K. H. (1997). What controls dissolved iron concentrations in the world ocean? *Marine Chemistry*, *57*(3–4), 137–161. https://doi.org/10.1016/s0304-4203(97)00043-1

Jørgensen, L., Stedmon, C. A., Kragh, T., Markager, S., Middelboe, M., & Søndergaard, M. (2011). Global trends in the fluorescence characteristics and distribution of marine dissolved organic matter. *Marine Chemistry*, *126*(1–4), 139–148. https://doi.org/10.1016/j.marchem.2011.05.002

Kim, T., Obata, H., Nishioka, J., & Gamo, T. (2017). Distribution of dissolved zinc in the western and central subarctic North Pacific. *Global Biogeochemical Cycles*, *31*(9), 1454–1468. https://doi.org/10.1002/2017gb005711

Kitayama, S., Kuma, K., Manabe, E., Sugie, K., Takata, H., Isoda, Y., et al. (2009). Controls on iron distributions in the deep water column of the North Pacific Ocean: Iron (III) hydroxide solubility and marine humic-type dissolved organic matter. *Journal of Geophysical Research*, *114*(C8), C08019. https://doi.org/10.1029/2008jc004754

Kondo, Y., Bamba, R., Obata, H., Nishioka, J., & Takeda, S. (2021). Distinct profiles of size-fractionated iron-binding ligands between the eastern and western subarctic Pacific. *Scientific Reports*, *11*(1), 2053. https://doi.org/10.1038/s41598-021-81536-6

Kondo, Y., Takeda, S., & Furuya, K. (2007). Distribution and speciation of dissolved iron in the Sulu Sean and its adjacent waters. *Deep-Sea Research II*, *54*(1–2), 60–80. https://doi.org/10.1016/j.dsr2.2006.08.019

Kuma, K., Nishioka, J., & Matsunaga, K. (1996). Controls on Iron (III) hydroxide solubility in seawater: The influence of pH and natural organic chelators. *Limnology & Oceanography*, *41*(3), 396–407. https://doi.org/10.4319/lo.1996.41.3.0396

Laglera, L. M., Battaglia, G., & van den Berg, C. M. G. (2007). Determination of humic substances in natural waters by cathodic stripping voltammetry of their complexes with iron. *Analytica Chimica Acta*, *599*(1), 58–66. https://doi.org/10.1016/j.aca.2007.07.059

Laglera, L. M., Sukekava, C., Slagter, H. A., Downes, J., Aparicio-Gonzalez, A., & Gerringa, L. J. A. (2019). First quantification of the controlling role of humic substances in the transport of iron across the surface of the Arctic Ocean. *Environmetal Science and Technology*, *53*(22), 13136–13145. https://doi.org/10.1021/acs.est.9b04240

Laglera, L. M., & van den Berg, C. M. G. (2009). Evidence for geochemical control of iron by humic substances in seawater. *Limnology & Oceanography*, *54*(2), 610–619. https://doi.org/10.4319/lo.2009.54.2.0610

Lam, P. J., & Bishop, J. K. B. (2008). The continental margin is a key source of iron to the HNLC North Pacific Ocean. *Geophysical Research Letters*, *35*(7), L07608. https://doi.org/10.1029/2008gl033294

Laurier, F. J. G., Mason, R. P., Gill, G. A., & Whalin, L. (2004). Mercury distributions in the North Pacific Ocean—20 yr of observations. *Marine Chemistry*, *90*(1–4), 3–19. https://doi.org/10.1016/j.marchem.2004.02.025

Liu, X., & Millero, F. J. (1999). The solubility of iron hydroxide in sodium chloride solutions. *Geochimica et Cosmochimica Acta*, *63*(19–20), 3487–3497. https://doi.org/10.1016/s0016-7037(99)00270-7

Lohan, M. C., & Bruland, K. W. (2008). Elevated Fe(II) and dissolved Fe in hypoxic shelf waters off Oregon and Washington: An enhanced source of iron to coastal upwelling regimes. *Environmental Science and Technology*, *42*(17), 6462–36468. https://doi.org/10.1021/es800144j

Martin, J. H., & Fitzwater, S. E. (1988). Iron deficiency limits phytoplankton growth in the north-east Pacific subarctic. *Nature*, *331*(6154), 341–343. https://doi.org/10.1038/331341a0

Misumi, K., Nishioka, J., Obata, H., Tsumune, D., Tsubono, T., Long, M. C., et al. (2021). Slowly sinking particles underlie dissolved iron transport across the Pacific Ocean. *Global Biogeochemical Cycles*, *35*(4), e2020GB006823. https://doi.org/10.1029/2020gb006823

Mopper, K., Zhou, X., Kieber, R. J., Kieber, D. J., Sikorski, R. J., & Jones, R. D. (1991). Photochemical degradation of dissolved organic carbon and its impact on the oceanic carbon cycle. *Nature*, *353*(6339), 60–62. https://doi.org/10.1038/353060a0

Morton, P. L., Landing, W. M., Shiller, A. M., Moody, A., Kelly, T. D., Bizimis, M., et al. (2019). Shelf inputs and lateral transport of Mn, Co, and Ce in the western North Pacific Ocean. *Frontiers in Marine Science*, *6*, 591. https://doi.org/10.3389/fmars.2019.00591

Nakatsuka, T., Toda, M., Kawamura, K., & Wakatsuchi, M. (2004). Dissolved and particulate organic carbon in the Sea of Okhotsk: Transport from continental shelf to ocean interior. *Journal of Geophysical Research*, *109*(C9), C09S14. https://doi.org/10.1029/2003jc001909

Nakatsuka, T., Yoshikawa, C., Toda, M., Kawamura, K., & Wakatsuchi, M. (2002). An extremely turbid intermediate water in the Sea of Okhotsk: Implication for the transport of particulate organic matter in a seasonally ice-bound sea. *Geophysical Research Letters*, *29*(16), 4-1–4-4. https://doi.org/10.1029/2001gl014029

Nishioka, J., Hirawake, T., Nomura, D., Yamashita, Y., Ono, K., Murayama, A., et al. (2021a). Iron and nutrient dynamics along the East Kamchatka Current, western Bering Sea Basin, and Gulf of Anadyr. *Progress in Oceanography*, *198*, 102662. https://doi.org/10.1016/j.pocean.2021.102662

Nishioka, J., Nakatsuka, T., Ono, K., Volkov, Y. N., Scherbinin, A., & Shiraiwa, T. (2014). Quantitative evaluation of iron transport processes in the Sea of Okhotsk. *Progress in Oceanography*, *126*, 180–193. https://doi.org/10.1016/j.pocean.2014.04.011

Nishioka, J., Nakatsuka, T., Watanabe, Y. W., Yasuda, I., Kuma, K., Ogawa, H., et al. (2013). Intensive mixing along an island chain controls oceanic biogeochemical cycles. *Global Biogeochemical Cycles*, *27*(3), 920–929. https://doi.org/10.1002/gbc.20088

Nishioka, J., & Obata, H. (2017). Dissolved iron distribution in the western and central subarctic Pacific: HNLC water formation and biogeochemical processes. *Limnology & Oceanography*, *62*(5), 2004–2022. https://doi.org/10.1002/lno.10548

Nishioka, J., Obata, H., Hirawake, T., Kondo, Y., Yamashita, Y., Misumi, K., & Yasuda, I. (2021b). A review: Iron and nutrient supply in the subarctic Pacific and its impact on phytoplankton production. *Journal of Oceanography*, *77*(4), 561–587. https://doi.org/10.1007/s10872-021-00606-5

Nishioka, J., Obata, H., Ogawa, H., Ono, K., Yamashita, Y., Lee, K. J., et al. (2020). Sub-polar marginal seas fuel the North Pacific through the intermediate water at the termination of the global ocean circulation. *Proceedings of the National Academy of Sciences of the United States of America*, *117*(23), 12665–12673. https://doi.org/10.1073/pnas.2000658117

Nishioka, J., Ono, T., Saito, H., Nakatsuka, T., Takeda, S., Yoshimura, T., et al. (2007). Iron supply to the western subarctic Pacific: Importance of iron export from the Sea of Okhotsk. *Journal of Geophysical Research*, *112*(C10), C10012. https://doi.org/10.1029/2006jc004055

Nishioka, J., Takeda, S., Kudo, I., Tsumune, D., Yoshimura, T., Kuma, K., & Tsuda, A. (2003). Size fractionated iron distributions and iron-limitation processes in the subarctic NW Pacific. *Geophysical Research Letters*, *30*(14), 1730. https://doi.org/10.1029/2002gl016853

Obata, H., Karatani, H., & Nakayama, E. (1993). Automated determination of iron in seawater by chelating resin concentration and chemiluminescence detection. *Analytical Chemistry*, *65*(11), 1524–1528. https://doi.org/10.1021/ac00059a007

Omori, Y., Hama, T., Ishii, M., & Saito, S. (2011). Vertical change in the composition of marine humic-like fluorescent dissolved organic matter in the subtropical western North Pacific and its relation to photoreactivity. *Marine Chemistry*, *124*(1–4), 38–47. https://doi.org/10.1016/j.marchem.2010.11.005

Resing, J. A., Sedwick, P. N., German, C. R., Jenkins, W. J., Moffett, J. W., Sohst, B. M., & Tagliabue, A. (2015). Basin-scale transport of hydrothermal dissolved metals across the South Pacific Ocean. *Nature*, *523*(7559), 200–203. https://doi.org/10.1038/nature14577

Romera-Castillo, C., Chen, M., Yamashita, Y., & Jaffé, R. (2014). Fluorescence characteristics of size-fractionated dissolved organic matter: Implications for a molecular assembly based structure? *Water Research*, *55*, 40–51. https://doi.org/10.1016/j.watres.2014.02.017

Stedmon, C. A., & Nelson, N. B. (2015). The optical properties of DOM in the ocean. In D. A. Hansell, & C. A. Carlson (Eds.), *Biogeochemistry of marine dissolved organic matter* (2nd ed., pp. 481–508). Academic Press.

Stolpe, B., Guo, L., Shiller, A. M., & Hassellöv, M. (2010). Size and composition of colloidal organic matter and trace elements in the Mississippi River, Pearl River, and the northern Gulf of Mexico, as characterized by flow field-flow fractionation. *Marine Chemistry*, *118*(3–4), 119–128. https://doi.org/10.1016/j.marchem.2009.11.007

Sutton, R., & Sposito, G. (2005). Molecular structure in soil humic substances: The new view. *Environmental Science and Technology*, *39*(23), 9009–9015. https://doi.org/10.1021/es050778q

Tagliabue, A., Aumont, O., & Bopp, L. (2014). The impact of different external sources of iron on the global carbon cycle. *Geophysical Research Letters*, *41*(3), 920–926. https://doi.org/10.1002/2013gl059059

Tagliabue, A., Bowie, A. R., Boyd, P. W., Buck, K. N., Johnson, K. S., & Saito, M. A. (2017). The integral role of iron in ocean biogeochemistry. *Nature*, *543*(7643), 52–59. https://doi.org/10.1038/nature21058

Tagliabue, A., Bowie, A. R., DeVries, T., Ellwood, M. J., Landing, W. M., Milne, A., et al. (2019). The interplay between regeneration and scavenging fluxes drives ocean iron cycling. *Nature Communication*, *10*(1), 4960. https://doi.org/10.1038/s41467-019-12775-5

Takata, H., Kuma, K., Iwade, S., Isoda, Y., Kuroda, H., & Senjyu, T. (2005). Comparative vertical distributions of iron in the Japan Sea, the Bering Sea, and the western North Pacific Ocean. *Journal of Geophysical Research*, *110*(C7), C07004. https://doi.org/10.1029/2004jc002783

Takata, H., Kuma, K., Iwade, S., Yamajyoh, Y., Yamaguchi, A., Takagi, S., et al. (2004). Spatial variability of iron in the surface water of the northwestern North Pacific Ocean. *Marine Chemistry*, *86*(3–4), 139–157. https://doi.org/10.1016/j.marchem.2003.12.007

Tani, H., Nishioka, J., Kuma, K., Takata, H., Yamashita, Y., Tanoue, E., & Midorikawa, T. (2003). Iron (III) hydroxide solubility and humic-type fluorescent organic matter in the deep water column of the Okhotsk Sea and the northwestern North Pacific Ocean. *Deep-Sea Research I, 50*(9), 1063–1078. https://doi.org/10.1016/s0967-0637(03)00098-0

Timko, S. A., Maydanov, A., Pittelli, S. L., Conte, M. H., Cooper, W. J., Koch, B. P., et al. (2015). Depth-dependent photodegradation of marine dissolved organic matter. *Frontiers in Marine Science*, *2*, 66. https://doi.org/10.3389/fmars.2015.00066

Uchida, R., Kuma, K., Omata, A., Ishikawa, S., Hioki, N., Ueno, H., et al. (2013). Water column iron dynamics in the subarctic North Pacific Ocean and the Bering Sea. *Journal of Geophysical Research*, *118*(3), 1257–1271. https://doi.org/10.1002/jgrc.20097

Velasquez, I. B., Ibisanmi, E., Maas, E. W., Boyd, P. W., Nodder, S., & Sander, S. G. (2016). Ferrioxamine siderophores detected amongst iron binding ligands produced during the remineralization of marine particles. *Frontiers in Marine Science*, *3*, 172. https://doi.org/10.3389/fmars.2016.00172

von der Heyden, B. P., & Roychoudhury, A. N. (2015). A review of colloidal iron partitioning and distribution in the open ocean. *Marine Chemistry*, *177*, 9–19. https://doi.org/10.1016/j.marchem.2015.05.010

Whitby, H., Bressac, M., Sarthou, G., Ellwood, M. J., Guieu, C., & Boyd, P. W. (2020a). Contribution of electroactive humic substances to the iron-binding ligands released during microbial remineralization of sinking particles. *Geophysical Research Letters*, *47*(7), e2019GL086685. https://doi.org/10.1029/2019gl086685

Whitby, H., Planquette, H., Cassar, N., Bucciarelli, E., Osburn, C. L., Janssen, D. J., et al. (2020b). A call for refining the role of humic-like substances in the oceanic iron cycle. *Scientific Reports*, *10*(1), 6144. https://doi.org/10.1038/s41598-020-62266-7

Whitby, H., & van den Berg, C. M. G. (2015). Evidence for copper-binding humic substances in seawater. *Marine Chemistry*, *173*, 280–290. https://doi.org/10.1016/j.marchem.2014.09.011

Wong, K., Nishoka, J., Kim, T., & Obata, H. (2022). Long-range lateral transport of dissolved manganese and iron in the subarctic Pacific. *Journal of Geophysical Research: Oceans*, *127*(2), e2021JC017652. https://doi.org/10.1029/2021jc017652

Wu, J., Boyle, E., Sunda, W., & Wen, L. S. (2001). Soluble and colloidal iron in the oligotrophic North Atlantic and North Pacific. *Science*, *293*(5531), 847–849. https://doi.org/10.1126/science.1059251

Yamashita, Y., Cory, R. M., Nishioka, J., Kuma, K., Tanoue, E., & Jaffé, R. (2010). Fluorescence characteristics of dissolved organic matter in the deep waters of the Okhotsk Sea and the northwestern North Pacific Ocean. *Deep-Sea Research II*, *57*(16), 1478–1485. https://doi.org/10.1016/j.dsr2.2010.02.016

Yamashita, Y., Nishioka, J., Obata, H., & Ogawa, H. (2020). Shelf humic substances as carriers for basin-scale iron transport in the North Pacific. *Scientific Reports*, *10*(1), 4505. https://doi.org/10.1038/s41598-020-61375-7

Yamashita, Y., & Tanoue, E. (2004). In situ production of chromophoric dissolved organic matter in coastal environments. *Geophysical Research Letters*, *31*(14), L14302. https://doi.org/10.1029/2004gl019734

Yamashita, Y., & Tanoue, E. (2008). Production of bio-refractory fluorescent dissolved organic matter in the ocean interior. *Nature Geoscience*, *1*(9), 579–582. https://doi.org/10.1038/ngeo279

Yamashita, Y., Tosaka, T., Bamba, R., Kamezaki, R., Goto, S., Nishioka, J., et al. (2021). Widespread distribution of allochthonous fluorescent dissolved organic matter in the intermediate water of the North Pacific. *Progress in Oceanography*, *191*, 102510. https://doi.org/10.1016/j.pocean.2020.102510

Yasuda, I., Hiroe, Y., Komatsu, K., Kawasaki, K., Joyce, T. M., Bahr, F., & Kawasaki, Y. (2001). Hydrographic structure and transport of the Oyashio south of Hokkaido and the formation of North Pacific Intermediate Water. *Journal of Geophysical Research*, *106*(C4), 6931–6942. https://doi.org/10.1029/1999jc000154

Yoshikawa, C., Nakatsuka, T., & Wakatsuchi, M. (2006). Distribution of N* in the Sea of Okhotsk and its use as a biogeochemical tracer of the Okhotsk Sea Intermediate Water formation process. *Journal of Marine Systems*, *63*(1–2), 49–62. https://doi.org/10.1016/j.jmarsys.2006.05.008